Article

Benchmarking Current Capabilities for the Generation of Excitation and Photoionisation Atomic Data

C A Ramsbottom *†, C P Ballance†, R T Smyth†, A Conroy†, L Fernández-Menchero†, M D Turkington† and F P Keenan‡

† Centre for Theoretical Atomic, Molecular and Optical Physics, School of Mathematics and Physics, Queen's University Belfast, Belfast BT7 1NN, UK

‡ Astrophysics Research Centre, School of Mathematics and Physics, Queen's University Belfast, Belfast BT7 1NN, UK

* Correspondence: c.ramsbottom@qub.ac.uk

Abstract: The spectra currently emerging from modern ground- and space-based astronomical instruments are of exceptionally high quality and resolution. To meaningfully analyse these spectra researchers utilise complex modelling codes to replicate the observations. The main inputs to these codes are atomic data such as excitation and photoionisation cross sections as well as radiative transition probabilities, energy levels and line strengths. In this publication the current capabilities of the numerical methods and computer packages used in the generation of these data are discussed. Particular emphasis is given to Fe-peak species and the heavy systems of tungsten and molybdenum. Some of the results presented to highlight certain issues and/or advances have already been published in the literature, while other sections present, for the first time, new recently evaluated atomic data.

Keywords: R-matrix; atomic data; atomic processes; collisions; Fe-peak elements; electron-impact excitation; photoionization

1. Introduction

The accurate determination of atomic data, both radiative and collisional, is essential for modelling and interpreting astronomical spectra. Current ground- and satellite-based instruments produce spectra of unprecedented quality and resolution, and the interpretation and analysis of these is crucially dependent on the quality and quantity of the atomic data available for incorporation into the spectroscopy modelling codes. Computational and numerical methods are considered the most viable approaches for producing the significant amounts of data required, as experimental techniques are often of insufficient accuracy or are limited to a small number of transitions. The research group at Queen's University Belfast has a longstanding and successful track record in the evaluation of these data, and have been directly involved in the development, testing, use and maintenance of all variants of the computational packages utilised to generate results. This publication will present a review of the current capabilities of the Belfast group, with regard to the quality of the collisional atomic data produced over the last number of years, the new atomic data now available for previously untreated ions, as well as the code development that has been undertaken to ensure that these calculations are tractable. Section 2 is devoted to a particular species of ion, the open d-shell Fe-peak elements, with particular emphasis given to the electron-impact excitation of singly ionised iron. In Section 3 we examine current advances in the generation of photoionisation cross sections and the quality of calculation that can now be performed. Finally in Section 4 we consider the heavier elements

of tungsten and molybdenum, of critical importance in fusion plasma research and thermonuclear reactors.

2. The Fe-peak elements

The Fe-peak elements constitute a unique group of ions that are critical in astrophysical applications. These niche elements, located in the periodic table from Sc (Z=21) through Zn (Z=30), provide one of the main keys to our understanding of the early Universe and star formation. Of particular interest are the low ionisation stages of elements such as Fe, Ni, Co, Cr and Mn, and atomic data for these are essential in the spectral modelling and analysis for a myriad of astronomical objects. It is very difficult to investigate these ions theoretically because of their open d-shell structures. Describing the target ion is problematic due to the hundreds of strongly coupled energy levels present, large numbers of coupled channels and the presence of numerous series of Rydberg resonances converging onto the target state thresholds in the low energy scattering domain. All of these have to be accurately accounted for in any calculation and the computational effort and capacity required is substantial. To overcome these problems, new parallel versions of the **R**-matrix computer packages have been developed over the years which can exploit both national and international HPC facilities. The Queen's University team have been involved in the development, testing and use of these new variants, ensuring that all our atomic calculations are carried out using the most up-to-date software.

As an indicator of the current capabilities for generating atomic data for these difficult species, we concentrate in this section on discussing the electron-impact excitation of singly ionised iron. Emission and absorption lines of Fe II have been identified in the spectra of objects as diverse as stars, planetary nebulae and quasars from the IR to the UV. Over the last thirty years many theorists have computed atomic data for this ion with little consensus found among the datasets (see Ramsbottom et al. [1] and [2] and references therein). These series of calculations have grown in complexity and size over the last decade, but no concrete evidence for convergence of the atomic data has been found. As an example we consider in Figure 1 the effective collision strength as a function of electron temperature for the spin-changing forbidden transition from the $3d^6 4s^6 D^e_{9/2}$ ground state of Fe II to the first metastable level above the ground state split levels, $3d^7\ ^4F^e_{9/2}$. This figure is from Ramsbottom et al [1] and displays the effective collision strengths generated by theoretical work from 1988 to 2007. The temperature of maximum abundance for Fe II in ionisation equilibrium is 10^4K, and at this temperature there are differences of a factor of 1.6 between the lowest and highest values of effective collision strength in Figure 1. There is closest agreement at the highest temperatures considered between the Ramsbottom et al [1] data (labelled present 262-level) and the much earlier and simpler evaluation of Berrington et al [3] (labelled Berr(88)). For temperatures below 1000K, the uncertainties for all calculations are greatest. The most sophisticated work in this figure is the Breit-Pauli calculation of Ramsbottom et al [1] which included 262 individual fine-structure levels corresponding to the $3d^6 4s$, $3d^7$ and $3d^6 4p$ configurations. Additional correlation effects were accounted for via the inclusion of a $\overline{4d}$ pseudo-orbital.

In an attempt to improve these data and to test their convergence, an additional two substantial evaluations have been completed recently by the Belfast group. The first was an extension of the Ramsbottom et al [1] Breit-Pauli model by incorporating all levels associated with the additional configurations $3d^5 4s^2$ and $3d^5 4s4p$. This gave rise to an extensive 716 fine-structure level calculation, generating data for over 250 000 individual transitions and dealing with 5076 coupled channels, the largest Fe II treatment undertaken to date. To test convergence we then performed a fully relativistic Dirac Atomic **R**-matrix calculation (DARC) including the original 262 levels (3 configurations) plus a further 17 configurations introduced as CI to provide a more accurate target model. In Figure 2 (a) we present the current comparison for the $3d^6 4s\ ^6D^e_{9/2}$ - $3d^7\ ^4F^e_{9/2}$ spin-changing transition, including the new 716 Breit-Pauli and 262 DARC evaluations. Close to the temperature of maximum abundance (10^4K), the BP-716, DARC-262 and the original data from Ramsbottom et al [1] agree to with 10%, and substantially better as we move to higher temperatures. Three very different models

Preprints (www.preprints.org) | NOT PEER-REVIEWED | Posted: 26 June 2018 doi:10.20944/preprints201806.0412.v1

Peer-reviewed version available at Galaxies 2018, 6, 90; doi:10.3390/galaxies6030090

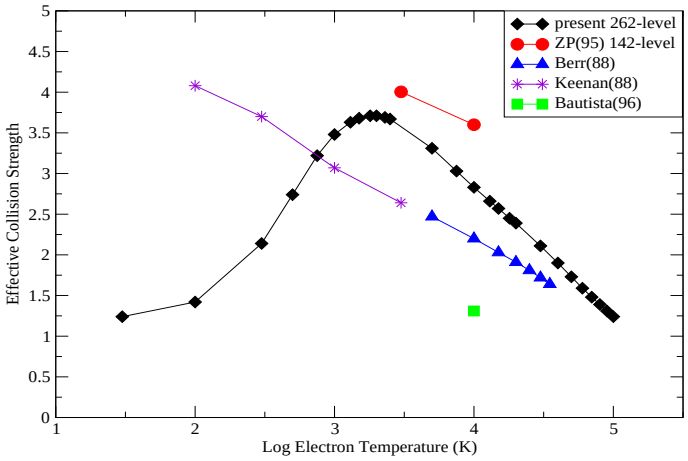

Figure 1. Effective Collision Strength as a function of log electron temperature in Kelvin for the $3d^6 4s\ ^6D^e_{9/2}$ - $3d^7\ ^4F^e_{9/2}$ fine-structure transition in Fe II: diamonds - 262 level calculation of [1], circles - 142 level calculation of [4], triangles - [3], stars - [5] and squares - [6]

using two different techniques are now producing similar effective collision strength values for the first time, across a range of temperatures, indicating that we are achieving near-convergence for this difficult-to-treat (yet vitally important) species. In Figure 2 (b) the mean of the three largest datasets is plotted and error bars produced to indicate their level of accuracy, facilitating future modelling for a wide range of astrophysical objects. It should be noted that a similar picture is found for many other important transitions with regard to comparison, accuracy, convergence and error prediction. A complete and comprehensive dataset of all effective collision strengths across a range of temperatures will be available from the authors in the near future.

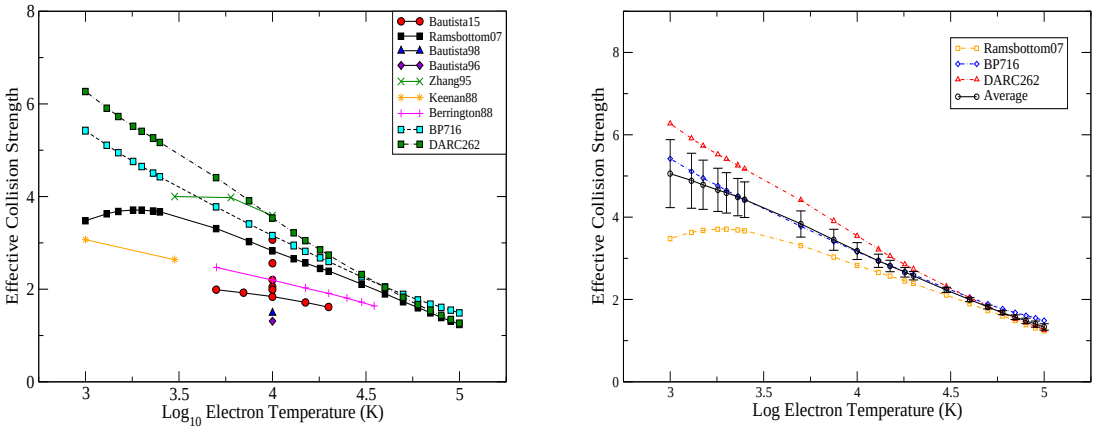

(a) **(b)**

Figure 2. (a) Effective Collision Strength as a function of log electron temperature in Kelvin for the $3d^6 4s\ ^6D^e_{9/2}$ - $3d^7\ ^4F^e_{9/2}$ fine-structure transition in Fe II: references [1], [4], [3], [5] and [6] as for Figure 1, BP716 - present 716 level Breit-Pauli calculation, DARC262 - present 262 level DARC calculation (b) black circles represent the mean of the three evaluations displayed.

Preprints (www.preprints.org) | NOT PEER-REVIEWED | Posted: 26 June 2018 doi:10.20944/preprints201806.0412.v1

Peer-reviewed version available at Galaxies 2018, 6, 90; doi:10.3390/galaxies6030090

3. Photoionisation Calculations

It is well known that massive stars and supernovae (SNe) play a critical role in galaxies. Through spectroscopic analysis we can deduce important parameters that describe these objects and obtain information on the evolutionary history of the star. Level-resolved photoionisation cross sections are essential data in the modelling codes and for many abundant ions in SNe, such as the Fe-peak elements already mentioned, these cross sections are not available. Difficulties arise in the evaluation of photoionisation cross sections due to the large intermediate dipole data files that need to be stored temporarily during the evaluations, leading to significant IO and memory issues. To overcome some of the computational bottlenecks, the Belfast group has undertaken some developments to the parallel **R**-matrix codes. The Breit-Pauli and DARC packages both employ two levels of MPI parallelisation, the first level is simply the distribution of distinct partial waves over processors concurrently, while the second level addresses the construction of the Hamiltonian matrix itself. Both the Breit-Pauli and DARC codes assign different numbers of processors to each Hamiltonian construction based upon its dimension. The goal is to reduce IO usage and hold the Hamiltonian matrix in memory.

We present in Figures 3 and 4 some examples of the quality of the photoionisation cross sections that can now be produced and the level of agreement that can be achieved when compared with experiment. Figure 3 shows partial cross sections for photoionisation of O-like S IX from the $2s^2 2p^4\ ^3P_2$ ground state to the four lowest final target levels, $2s^2 2p^3\ ^4S^o_{3/2}$, $^2D^o_{3/2,5/2}$ and $^2P^o_{1/2}$, see Tyndall et al [7]. Comparisons are provided in the figure with a limited set of resonance-free data obtained from the OPEN-ADAS database. Excellent agreement is evident for all four partial cross sections at all photon energies, and the Rydberg resonances converging onto the target thresholds are clearly and carefully resolved.

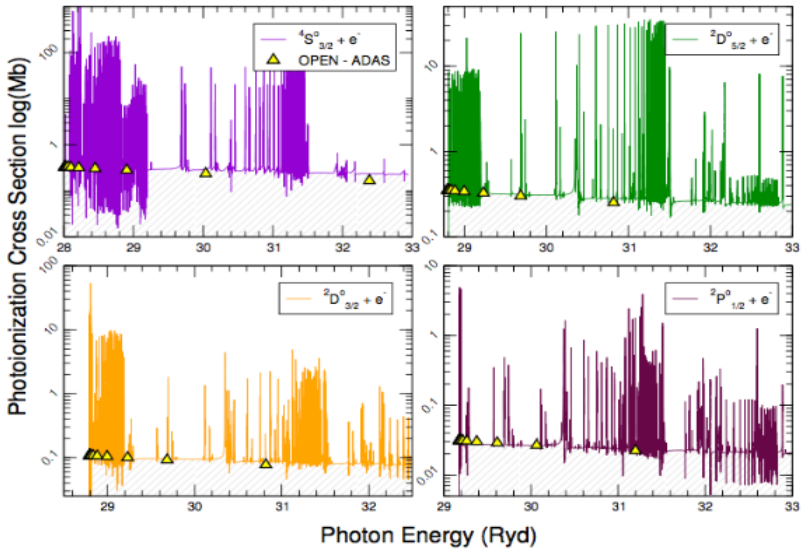

Figure 3. The partial photoionisation cross section contributions from transitions from the $^3P_2$ ground state of O-like S IX to the lowest 4 final target levels ($^4S^o_{3/2}$, $^2D^o_{3/2,5/2}$, $^2P^o_{1/2}$). Solid line [7], triangles OPEN-ADAS database.

In Figure 4 (a) we present the total photoionisation cross section from the initial $3s^2 3p^5\ ^2P^o$ ground state of Cl-like Ar II from Tyndall et al [8]. Two Breit-Pauli as well as a large fully relativistic DARC

calculation are shown in the figure and compared with absolute cross sections obtained from the merged beam apparatus at the Advanced Light Source (ALS) at an energy resolution of 10meV [9]. Excellent agreement is found at all photon energies considered, with particularly good conformity in the low energy region close to threshold, and in the vicinity of the Cooper minimum around 45eV. To further emphasise the exceptional quality of the data we can now produce, we expand in Figure 4 (b) the photon energy region just above threshold, from 27.8 - 29.2 eV. Across this very narrow range exceptional conformity is achieved, indicating how accurately the theory and numerical methods can mirror the experimental values.

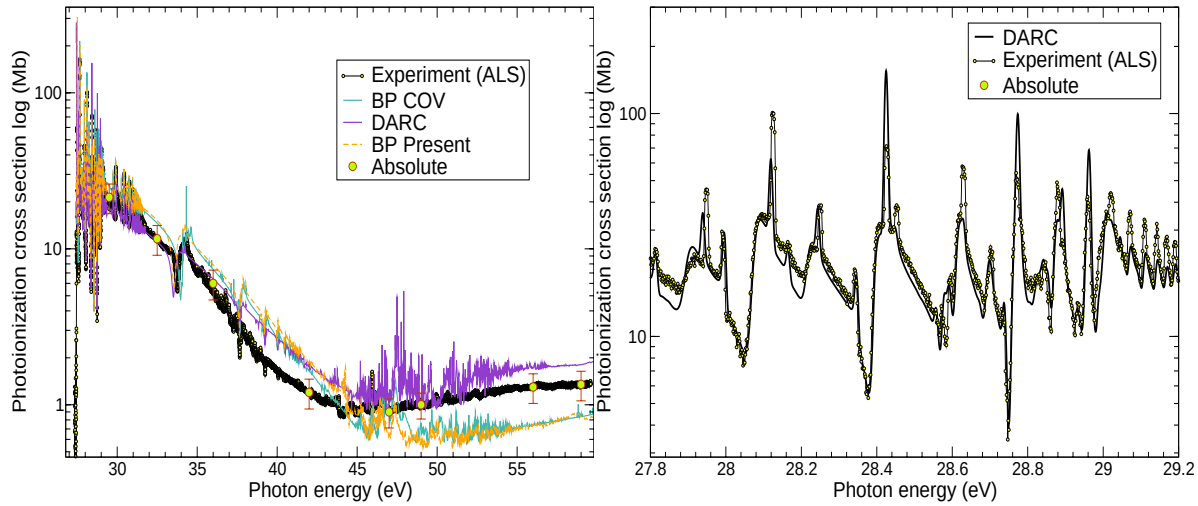

Figure 4. (a) Total photoionisation cross section for the ground $^2P^o$ state of Cl-like Ar II. Circles - experimental measurements of [9], solid purple DARC evaluations of [8], dashed orange Breit-Pauli calculation of [8]; (b) Total photoionisation cross section for the ground $^2P^o$ state of Cl-like Ar II between 27.8-29.2 eV just above threshold. Solid black line is the DARC calculation of [8] and the yellow circles are the experimental values of [9]

4. Heavier Systems

Atomic data for heavy elements such as tungsten and molybdenum have wide applications in areas such as fusion energy and plasma physics. For example, neutral tungsten is well known to be the primary candidate for lining the wall of the divertor region of the International Thermonuclear Experimental Reactor (ITER), while neutral molybdenum is extensively used as a plasma facing component (PFC) in tokamaks. Similar to the Fe-peak elements, these complex atoms and ions are very difficult to model due to the presence of a half-open 4d sub-shell in the ground state representation of Mo I, and a half-filled 5d sub-shell in the case of W I. Additional complications arise in the diagnostics due to the misidentification of lines and an absence of classification for many states in the spectral database for these ions. Strong mixing between low lying levels, of which there are many hundreds, makes it very difficult to model these ions and obtain a reasonable structure representation for use in the collisional calculations.

To allow these substantial projects to be tractable, the computational capacity of the relativistic DARC **R**-matrix packages needed to be upgraded and some code development was required. Our recent DARC collisional calculations for neutral heavy systems have adopted more extensive large-scale atomic structure models, including up to 25 target configurations, which results in up to 7825 fine-structure levels and 62917 relativistic configurations (MXNC). However, integer arrays associated

Preprints (www.preprints.org) | NOT PEER-REVIEWED | Posted: 26 June 2018 doi:10.20944/preprints201806.0412.v1

Peer-reviewed version available at Galaxies 2018, 6, 90; doi:10.3390/galaxies6030090

with angular algebra calculations within the DARC codes require dimensions of up to MXNC $\times$ (MXNC -1), a value which exceeds the capabilities of integer*4 precision for MXNC $>$ 46341. As a result, recent upgrades to our set of DARC codes include the option to modify all relevant integer values to integer*8 precision during calculations, and also leave the integer*4 precision of all passing binary files unchanged to interface with other existing R-matrix codes. Additional dimension checks and dynamic array allocations during runtime have also been implemented for angular algebra arrays throughout the DARC codes. This alleviates the need for setting fixed parameters for array allocation prior to compilation, which previously may have resulted in termination at a late point in the calculation if they were not sufficiently large. Now, once the limit of the array dimension is reached, a new routine will employ intrinsic Fortran 2003 subroutine calls to carry out a fast binary allocate/deallocate, recreating the angular algebra array with increased dimensions and preserving the original contents, ultimately minimising the computational cost.

Following these developments some very impressive atomic data have been compiled by the Belfast group for Mo I and W I. In Figures 5 (a) and (b) we present the electron-impact excitation cross sections for the $a\ ^7\mathrm{S} \rightarrow z\ ^7\mathrm{P^o}$ (390.3nm, 386.4nm, 379.8nm) and $a\ ^5\mathrm{S} \rightarrow z\ ^5\mathrm{P^o}$ (557.0nm, 553.3nm, 550.6nm) important diagnostic lines of Mo I as a function of incident electron energy from Smyth et al [10] and references therein. Comparisons are made with the earlier (and less sophisticated) work of Badnell et al [11] and Bartschat et al [12]. It is evident in both figures that the current excitation cross sections are much smaller in magnitude than those previously predicted, although we see good agreement with regard to shape. To demonstrate the quality and accuracy of this dataset we present in Figure 6 the photon emissivity coefficients (PECs) calculated using the improved results in the 379-391 and 550-558nm ranges, and compare with the observed spectrum obtained by the Compact Toroidal Hybrid plasma experiment (CTH) at Auburn University [13]. A high level of agreement is clearly evident across both wavelength regions, providing support for the accuracy of the atomic data produced.

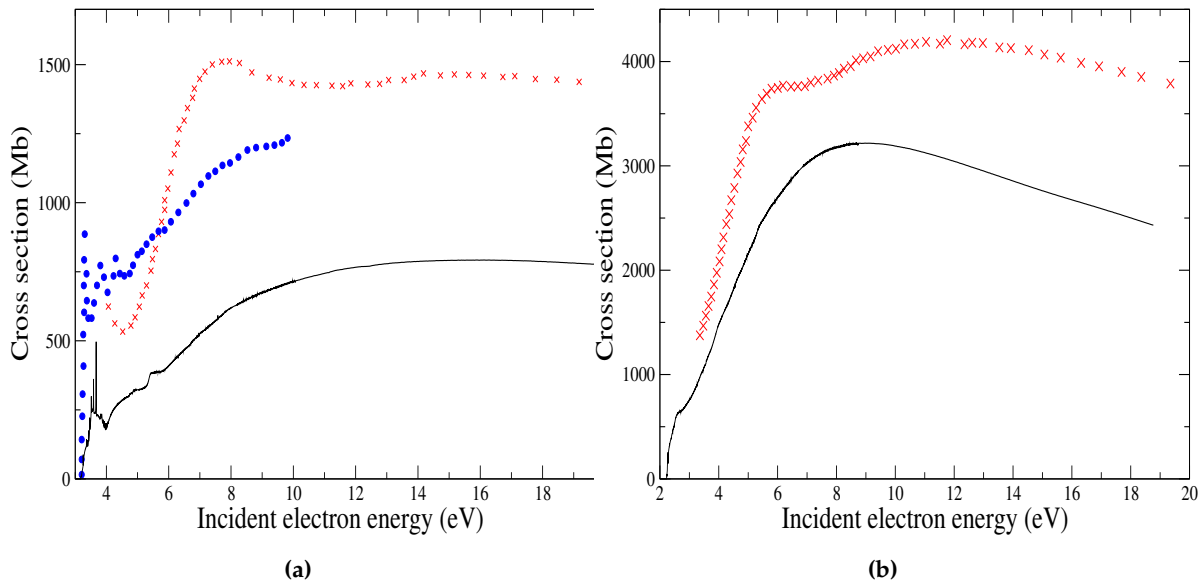

Figure 5. (a) The $a\ ^7\mathrm{S} \rightarrow z\ ^7\mathrm{P^o}$ excitation cross section in Mo I. The black curve is from [10], red crosses from [11] and blue circles from [12]: (b) The $a\ ^5\mathrm{S} \rightarrow z\ ^5\mathrm{P^o}$ excitation cross section in Mo I. The black curve is from [10], red crosses from [11]

In Figures 7 and 8 we present similar evidence of accuracy and quality for neutral tungsten, with data from Smyth et al [14]. Figure 7 shows effective collision strengths for four diagnostically important transitions in W I and a comparison with a less sophisticated plane-wave Born calculation,

Preprints (www.preprints.org) | NOT PEER-REVIEWED | Posted: 26 June 2018 doi:10.20944/preprints201806.0412.v1

Peer-reviewed version available at Galaxies 2018, 6, 90; doi:10.3390/galaxies6030090

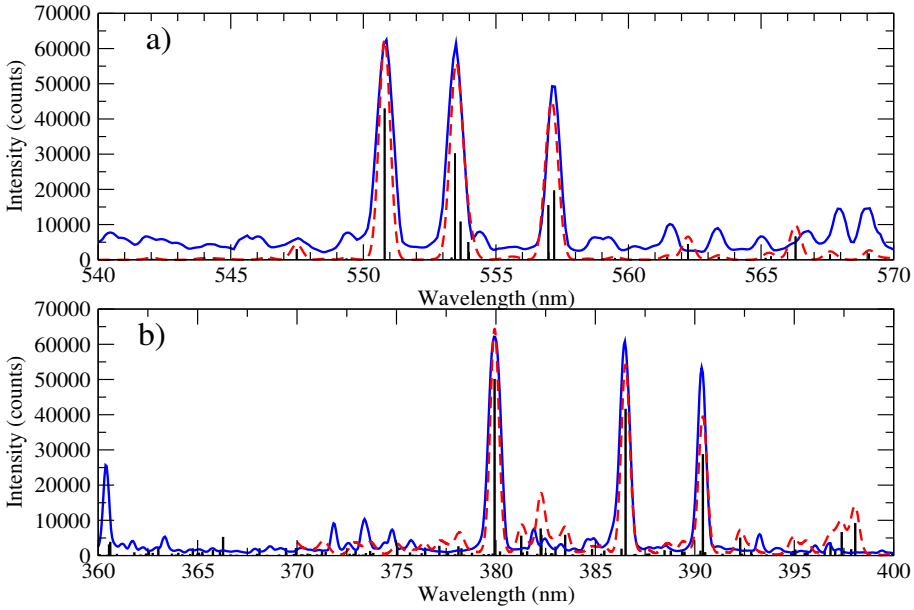

Figure 6. Measured spectra from the CTH plasma (solid blue line) [13] compared with the theoretical results from [10] (dashed red)

while Figure 8 contains the spectrum from the CTH experiment compared with those generated using these new atomic data. Excellent agreement is again evident for the well-known diagnostic lines at 400.88nm, 410.21nm and 430.21nm, with respect to both magnitude and position.

The remainder of this section concentrates on the structure packages that are currently available for use within the **R**-matrix framework, and whether one lends itself more appropriately when dealing with these complicated ions. Structure packages considered are the semi-relativistic configuration interaction CIV3 code [16], the semi-relativistic autostructure (AS) package [17] and finally the fully-relativistic GRASP structure code [18]. The first two are commonly used alongside the Breit-Pauli suite of **R**-matrix codes, and the latter with the DARC packages. In Figures 9 (a) and (b) we present collision strengths and the corresponding Maxwellian-averaged effective collision strength for the spin-changing $4s^2\ ^1S_0 \rightarrow 4s4p^3P^o_1$ forbidden transition in highly ionised W $^{44+}$. This important line is reasonably strong but couples closely to the $^1P^o$ terms in the expansion and hence correlation and mixing effects will be important. In Figure 9 (a) three calculations are presented using CIV3 and AS orbital parameters and configuration sets varying in size from 14 to 27. The resonance profiles align quite well but differ slightly in position and magnitude at some incident electron energies. This does not appear to significantly affect the corresponding effective collision strengths plotted in Figure 9 (b) for these three models, and the atomic data are in excellent agreement for all temperatures considered. Both of these structure packages work in a semi-relativistic regime, and for highly ionised heavy systems such as W^{44+} relativistic effects become increasingly important. To test this we present in Figure 9 (b) the rates produced by a full relativistic GRASP structure treatment with varying size of model from 13 to 22 configurations. at the high temperatures above 10^7K, all 5 calculations exhibit excellent agreement, with slightly larger disparities appearing at the lowest temperatures considered ($\approx$ 10^6K). Nonetheless, it is very encouraging to see the conformity of the structure and collision codes when treating these highly ionised heavy species. These data will be useful in applications to magnetically confined fusion plasmas and will help characterise useful diagnostic lines and identify the influx of potential impurities into the plasma core.

Acknowledgments: The work presented in this publication has been supported by funding from the STFC ST/P000312/1 QUB Astronomy Observation and Theory Consolidated grant and from the ADAS consortium EUF P7 funding agency. All calculations were carried out on either the Cray XC40 'Hazelhen' supercomputer in HLRS Stuggart, ARCHER at UCL or the Cray XC40 'Cori' supercomputer at NERSC California. .

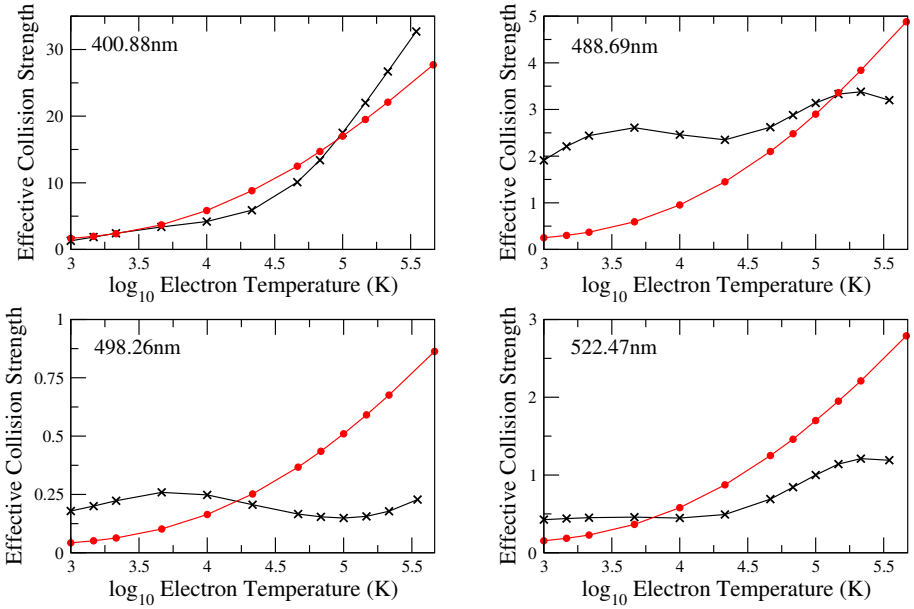

Figure 7. Effective collision strengths for the $5d^4 6s6p\ {}^7P^o_4 \rightarrow 5d^5 6s\ {}^7S_3$ (400.88nm), $5d^4 6s6p\ {}^7F^o_5 \rightarrow 5d^4 6s^2\ {}^5D_4$ (488.69nm), $5d^4 6s6p\ {}^7F^o_1 \rightarrow 5d^4 6s^2\ {}^5D_0$ (498.26nm) and $5d^4 6s6p\ {}^7D^o_2 \rightarrow 5d^4 6s^2\ {}^5D_3$ (522.47nm) transitions in W I. Solid black line with crosses are from [14] and the redline with dots are from a plane-wave Born calculation based on calculations by [15].

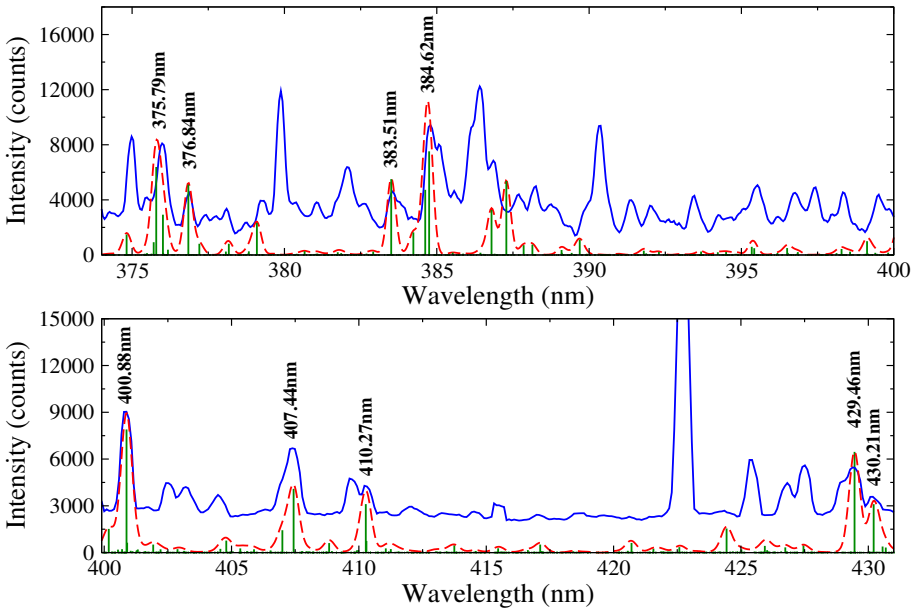

Figure 8. Observed spectrum from the CTH experiment (solid blue line) compared to the theoretical data of [14] (red dashed line).

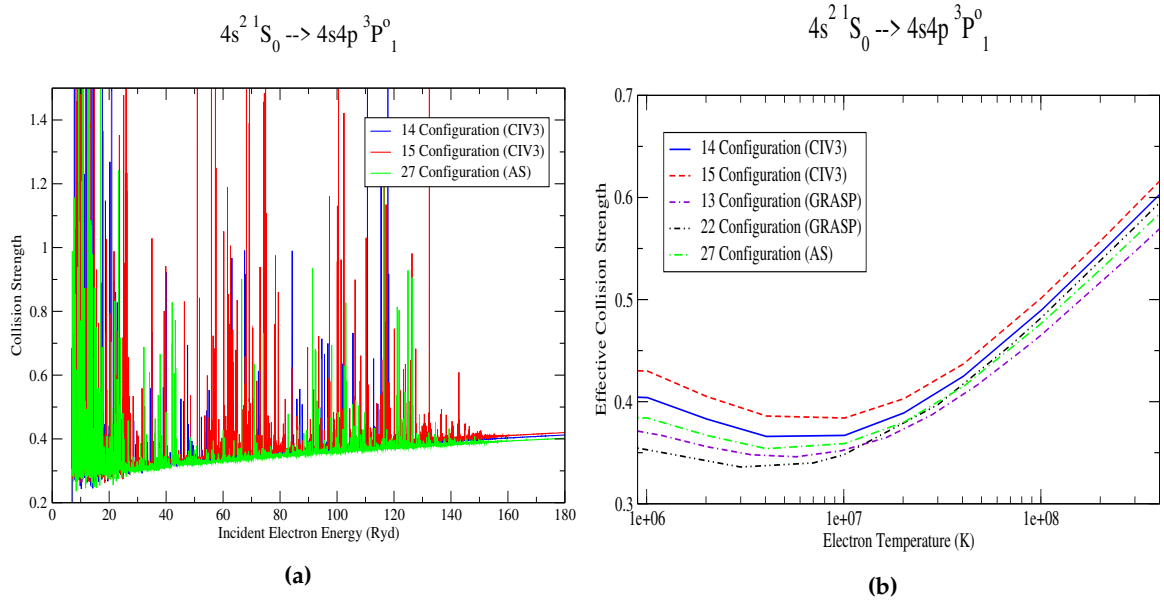

Figure 9. (a) The collision strength as a function of incident electron energy (in Ryds) for the $4s^2\ ^1S_0 \rightarrow 4s4p\ ^3P^o_1$ transition in W^{44+} and (b) the corresponding Maxwellian averaged effective collision strength as a function of electron temperature in Kelvin. This data has yet to be published.

References

1. Ramsbottom C A, Hudson C E, Norrington P H and Scott M P *Astron. & Astrophys.* **2007**, *475*, 765-769.
2. Ramsbottom C A *Atomic Data and Nuclear Data Tables* **2009**, *95*, 910-986.
3. Berrington K A, Burke P G, Hibbert A, Mohan M and Baluja K L *J.Phys.B.At.Mol.Opt.Phys* **1988**, *21*, 339.
4. Zhang H L and Pradhan A K *A&A* **1995**, *293*, 953.
5. Keenan F P, Hibbert A, Burke P G and Berrington K A *ApJ* **1988**, *332*, 539.
6. Bautista M A and Pradhan A K *A&AS* **1996**, *115*, 551.
7. Tyndall N B, Ramsbottom C A, Hibbert A and Ferland G *J.Phys.B:At.Mol.Opt.Phys.* **2015**, *48*, 155204.
8. Tyndall T B, Ramsbottom C A, Ballance C P and Hibbert A *MNRAS* **2016**, *456*, 366-373.
9. Covington A M et al *Phys.Rev.A* **2011**, *84*, 013413.
10. Smyth R T, Johnson C A, Ennis D A, Loch S D, Ramsbottom C A and Ballance C P *Phys.Rev.A* **2017**, *96*, 042713.
11. Badnell N R, Gorczyca T W, Pindzola M S and Summers H P *J.Phys.B:At.Mol.Opt.Phys.* 1996, *29*, 3683.
12. Bartschat K, Dasgupta A and Giuliani J L *J.Phys.B:At.Mol.Opt.Phys.* **2002**, *35*, 2899.
13. Hartwell G J, Knowlton S F, Hanson J D, Ennis D A and Maurer D A *Fusion Sci.Technol.* **2017**, *72*, 76.
14. Smyth R T, Ballance C P, Ramsbottom C A, Johnson C A, Ennis D A and Loch S D *Phys.Rev.A* **2018**, 052705.
15. Quinet P, Palmeri P and Biémont É *J.Phys.B:At.Mol.Opt.Phys.* **2011**, *44* 145005.
16. Hibbert A *Comput.Phys.Commun* **1975**, *9*, 141.
17. Badnell N R *J.Phys.B:At.Mol.Opt.Phys.* **1986**, *19*, 3827.
18. Parpia F A, Fischer C F and Grant I P *Comput.Phys.Commun* **1996**, *94*, 249.